EAGr: Supporting Continuous Ego-centric Aggregate Queries over Large Dynamic Graphs

Jayanta Mondal Amol Deshpande

Dept. of Computer Science, University of Maryland, College Park, MD 20742
{jayanta, amol}@cs.umd.edu

ABSTRACT

In this paper, we present EAGr, a system for supporting large numbers of continuous neighborhood-based ("ego-centric") aggregate queries over large, highly dynamic, rapidly evolving graphs. Examples of such queries include computation of *personalized, tailored trends* in social networks, *anomaly or event detection* in communication or financial transaction networks, *local search* and *alerts* in spatio-temporal networks, to name a few. Key challenges in supporting such continuous queries include very high update rates typically seen in these situations, large numbers of queries that need to be executed simultaneously, and stringent low latency requirements. We propose a flexible, general, extensible in-memory framework for executing different types of ego-centric aggregate queries over large dynamic graphs with low latencies. Our framework is built around the notion of an *aggregation overlay graph*, a pre-compiled data structure that encodes the computations to be performed when an update or a query is received. The overlay graph enables *sharing of partial aggregates* across different ego-centric queries (corresponding to different nodes in the graph), and also allows *partial pre-computation* of the aggregates to minimize the query latencies. We present several highly scalable techniques for constructing an overlay graph given an aggregation function, and also design incremental algorithms for handling changes to the structure of the underlying graph itself. We also present an optimal, polynomial-time algorithm for making the pre-computation decisions given an overlay graph. Although our approach is naturally parallelizable, we focus on a single-machine deployment and show that our techniques can easily handle graphs of size up to 320 million nodes and edges, and achieve update and query throughputs of over 500,000/s using a single, powerful machine.

Categories and Subject Descriptors

H.2.4 [**Database Management**]: Systems—*Query Processing*

Keywords

Graph databases; Continuous queries; Aggregates; Data streams; Ego-centric analysis; Graph compression; Social networks

SIGMOD '14, June 22-27, 2014, Snowbird, Utah, USA.
Copyright 2014 ACM 978-1-4503-2376-5/14/06 ...$15.00.

1. INTRODUCTION

Graph-structured data arises naturally in a variety of application domains, including social networks, communication networks, phone call networks, email networks, financial transaction networks, to name a few. There is an increasing need to support graph structure-aware queries and analysis tasks over such graphs, leading to much work in this area over the last few years. In many of these domains, the datasets are not only large in terms of the sheer number of nodes and edges in the graph, but they also produce a large amount of data at a very high rate, generating a *data stream* that must be ingested and queried in real time. The graph data can be seen as comprising of two major components: (a) a graph (*network*) component that captures the underlying interconnection structure among the nodes in the graph, and (b) *content* data associated with the nodes and the edges. The graph data stream contains updates to both these components. The structure of the graph may itself change rapidly in many cases, especially when things like webpages, user tags (e.g., Twitter *hashtags*), financial trades, etc., are treated as nodes of the graph. However, most of the data stream consists of updates to the content data associated with the nodes and edges, e.g., status updates or photos uploaded by social network users, phone calls or messages among users, transactions in a financial network, etc. Real-time, continuous query processing over such dynamic graph-structured data has become a critical need in the recent years.

In this paper, we focus on a prevalent class of queries over dynamic graphs, called *neighborhood-based or ego-centric aggregate queries*. In an ego-centric aggregate query, the querier (called *user* henceforth) corresponds to a node in the graph, and is interested in an aggregate over the current state or the recent history of a local neighborhood of the node in the graph; such local neighborhoods are often called *ego networks* of the nodes [25, 15]. An example of such a query is *ego-centric trend analysis in social networks* where the goal is to find, for each user, the trends (e.g., popular topics of discussion, news items) in his or her local neighborhood [1, 17]. The neighborhood here could be 1-hop neighborhood, or could extend beyond that. Similarly, in a phone-call network or an analogous communication network, we may be interested in identifying interesting events or anomalies (e.g., higher than normal communication activity among a group of nodes); that often boils down to continuously computing ego-centric aggregates over recent activity in a large number of local neighborhoods simultaneously (with an anomaly defined by a predicate on the aggregate) [2, 29]. In spatio-temporal social networks, users are often interested in events happening in their social networks, but also physically close to them.

We make a distinction between between *continuous* queries and what we call *quasi-continuous* queries (somewhat surprisingly, we have not seen this distinction made in prior work). In the latter case, the query result only needs to produced or updated when the user requests it (we call such user requests *reads*); whereas in the former case, the query result must be kept up-to-date whenever the inputs change. The first query above (trend analysis) is an example of a quasi-continuous query since there is no need to produce the result unless the user asks for it (for reducing latency, full or partial pre-computation may be performed). However, anomaly detection queries must be executed continuously as new updates arrive.

The high update rates typically seen in these application domains make it a challenge to execute a large number of such queries with sufficiently low latencies. A naive *on-demand* approach, where the neighborhood is traversed in response to a read, is unlikely to scale to the large graph sizes, and further, would have unacceptably high query latencies. On the other hand, a *pre-computation-based approach*, where the required query answers are always pre-computed and kept up-to-date will likely lead to much wasted computation effort for most queries. Furthermore, both these approaches ignore many potential optimization opportunities, in particular, the possibility of *sharing* the aggregate computation across different queries (corresponding to different ego networks).

In this paper, we propose an approach that maintains a special directed graph (called an *aggregation overlay graph* or simply an *overlay*) that is constructed given an ego-centric aggregate query and a subset of nodes in the data graph for which it needs to be evaluated continuously (or quasi-continuously). The overlay graph exposes sharing opportunities by explicitly utilizing *partial aggregation* nodes, whose outputs can be shared across queries. The nodes in the overlay are labeled with *dataflow decisions* that encode whether data should be *pushed* to that node in response to an update, or it should be *pulled* when a query result needs to be computed. During execution, the overlay simply reacts to the events (i.e., reads and writes) based on the encoded decisions, and is thus able to avoid unnecessary computation, leading to very high throughputs across a spectrum of workloads. Constructing the optimal overlay graph is NP-Hard for arbitrary graph topologies. Further, given the large network sizes that are typically seen in practice, it is infeasible to use some of the natural heuristics for solving this problem. We present a series of highly efficient overlay construction algorithms and show how they can be scaled to very large graphs. Surprisingly, the problem of making the dataflow decisions for a given overlay is solvable in polynomial time, and we present a *max-flow*-based algorithm for that purpose. Our framework can support different neighborhood functions (i.e., 1-hop, 2-hop neighborhoods), and also allows filtering neighborhoods (i.e., only aggregating over subsets of neighborhoods). The framework also supports a variety of aggregation functions (e.g., *sum, count, min, max, top-k*, etc.), exposes an aggregation API for specifying and executing arbitrary user-defined aggregates. We conduct a comprehensive experimental evaluation over a collection of real-world networks, our results show that overlay-based execution of aggregation queries saves redundant computation and significantly boosts the end-to-end throughput of the system.

Outline: We begin with a brief overview of the problem by discussing the data and the query model (Section 2). Then we present the details of our proposed aggregation framework. Next we analyze the optimization problem of constructing an *overlay graph* (Section 3), and propose several scalable heuristics. Following that, we discuss how we make the dataflow (push/pull) decisions to minimize data movement in the overlay (Section 4). Then we describe our experimental setup and present a comprehensive experimental evaluation (Section 5), and discuss some of the most related work (Section 6).

Notation	Description
$\mathcal{G}(V, E)$	Underlying data graph
$\mathcal{N}()$	Neighborhood selection function
$\mathcal{F}()$	Aggregate function
write on v	An update to node v's content
read on v	A read to query result at v, i.e., $\mathcal{F}(\mathcal{N}(v))$
$A_\mathcal{G}(V', E')$	Bipartite directed writer/reader graph: for each node $v \in \mathcal{G}(V, E)$, it contains two nodes v_w (writer) and v_r (reader), with edges going from writers to readers
$O_\mathcal{G}(V'', E'')$	Overlay Graph
$\mathcal{I}(ovl)$	Set of writers aggregated by overlay node ovl
$w(v)$	write frequency of node v
$r(v)$	read (query) frequency of node v
$f_h(v)$	push frequency of node v in an overlay
$f_l(v)$	pull frequency of node v in an overlay

Table 1: Notation

2. OVERVIEW

We start with describing the underlying data and query model, followed by an overview of our proposed aggregation framework.

2.1 Data and Query Model

Data Model: Let $\mathcal{G}(V, E)$ denote the underlying connection graph, with V and E denoting the sets of nodes and edges respectively. In general, $\mathcal{G}$ is a heterogeneous, multi-relational graph that may contain many different types of nodes and may contain both directed and undirected edges. For example, for a social network, we may have nodes representing the users of the network as well as nodes representing communities, groups, user tags, webpages, and so on. Similarly, E may include not only symmetric *friendship* (or analogous) edges but also asymmetric *follows* edges, *membership* edges, and other types of semi-permanent edges that are usually in existence from the time they are formed till the time they are deleted (or till the current time). The *content* associated with the nodes and edges is captured through a set of *attribute-value* pairs.

We capture the structure updates (i.e., node or edge additions or deletions) as a time-stamped data stream $S_\mathcal{G}$ (called *structure data stream*). For simplicity, we assume that all the content is associated with nodes, and for a node v, we capture the content updates associated with it as a time-stamped data stream, S_v (called *content data streams*). We further assume that all the content streams are homogeneous, i.e., all updates are of the same type or refer to the same attribute. It is straightforward to relax both these assumptions. A content update on node v is also called a *write on* v.

Unlike most prior work in data streams or publish-subscriber networks where the producers of data (i.e., writers) and the consumers of data (i.e., readers) are distinct from each other, in our case, a node acts both as a writer and a reader. Hence, for clarity of description, when referring to a node v in the rest of the paper, we often denote its role in the context using a subscript – v_w (similarly, v_r) denoting the node as a writer (reader).

Query Model: An ego-centric aggregate query is specified by four parameters: $\langle \mathcal{F}, w, \mathcal{N}, pred \rangle$, where $\mathcal{F}$ denotes the aggregate function to be computed, w denotes a sliding window over the content data streams, $\mathcal{N}$ denotes the neighborhood selection function (i.e., $\mathcal{N}(v)$ forms the input list to be aggregated for each v), and $pred$ selects a subset of V for which the aggregate must be computed (i.e., $\mathcal{F}$ would be computed for all nodes for which $pred(v)$ is *true*). Following the data streams literature, w may be a time-based sliding window or a tuple-based sliding window; in the former case, we are given a time interval T, and the updates that arrive within the last T time are of interest, whereas in the latter case, we are given a number c, and the last c updates are of interest. The query may be specified to be a *continuous* query or a *quasi-continuous* query. For a continuous query, the query results must be kept up-to-date as

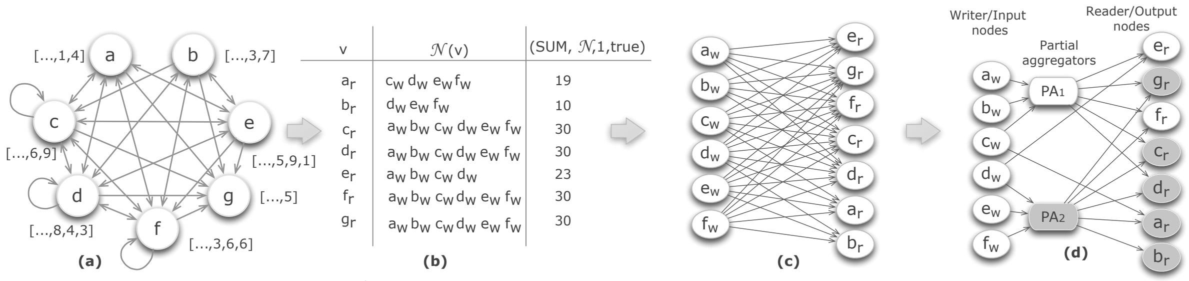

v	$\mathcal{N}$(v)	(SUM, $\mathcal{N}$,1,true)
a_r	c_w d_w e_w f_w	19
b_r	d_w e_w f_w	10
c_r	a_w b_w c_w d_w e_w f_w	30
d_r	a_w b_w c_w d_w e_w f_w	30
e_r	a_w b_w c_w d_w	23
f_r	a_w b_w c_w d_w e_w f_w	30
g_r	a_w b_w c_w d_w e_w f_w	30

Figure 1: (a) An example data graph, (b) $\mathcal{N}(v)$ and SUM aggregates for each v, (c) Bipartite representation of the graph, i.e, $A_{\mathcal{G}}$ (note, g does not form input to any reader), (d) An overlay graph (shaded nodes indicate *pull* decisions, unshaded ones indicate *push*).

new updates arrive, whereas for a quasi-continuous query, the query result for a node v is only needed when a user requests it (we call this a *read on* v); in the latter case, pre-computation may be done to reduce not only user latencies but also total computational effort.

Since our approach is based on pre-computation and maintenance of partial aggregates, we assume that the aggregate function (and $\mathcal{N}$) are pre-specified. In some cases, it is possible to share the intermediate data structures and partial aggregates for simultaneous evaluation of different aggregates; we do not consider that option further in this paper. Our system supports a set of built-in aggregate functions like *sum, max, min, top-k, etc.*, and we allow the user to define arbitrary aggregation functions (Section 2.2.3). Our system treats $\mathcal{F}$ as a blackbox, but the user may optionally specify whether the aggregation function is *duplicate-insensitive* or supports efficient *subtraction* (Section 3.1), and that information will be used to further optimize the computation.

Example: Figure 1 shows an example instance of this problem. Figure 1(a) depicts the data graph. $\mathcal{N}(x)$ is defined to be $\{y|y \rightarrow x\}$ (note that, all edges are not bidirectional). The numbers in the square brackets denote individual content streams. For example, there have been two *recent writes* on node a with values 1 and 4. The query is $\langle \text{SUM}, c = 1, \mathcal{N}, v \in V\rangle$, which states that for each node $v \in V$, the most recent values written by nodes in $\mathcal{N}(v)$ need to be aggregated using SUM. Figure 1(b) enumerates $\mathcal{N}(v)$ for each v. The last column of Figure 1(b) shows the results of the *read* queries on each node. For example, here $\mathcal{N}(a)$ evaluates to $\{c, d, e, f\}$, and a *read* query on a returns: $(9) + (3) + (1) + (6) = 19$. Figure 1(c) represents the corresponding directed bipartite graph $A_{\mathcal{G}}$ where nodes are duplicated and divided based on their roles; a node might or might not play both the roles.

Scope of the Approach: Here, we briefly summarize the key assumptions that we make and the limitations of our approach. Our compilation-based approach requires upfront knowledge of the query to be executed, including the specific aggregate function, the neighborhood to aggregate over, and the sliding window parameters (the last of which only impacts dataflow decisions). Further, given the high overlay construction cost, the query needs to be evaluated continuously for a period of time to justify the cost. Thus our approach would not be suitable for ad hoc ego-centric aggregate queries over graphs. We also note that, although our framework can handle arbitrary aggregation functions, the benefits of our approach, especially of sharing partial aggregates, are higher for *distributive* and *algebraic* aggregates than for *holistic* aggregates like *median*, *mode*, or *quantile* (however, approximate versions of holistic aggregates can still benefit from our optimizations). Our approach to making dataflow decisions based on expected read/write frequencies also requires the ability to estimate or predict those frequencies. As with most workload-aware approaches, our approach will likely not work well in face of highly unpredictable and volatile workloads. Finally, we also assume that the data graph itself changes relatively slowly; although we have developed incremental techniques to modify the overlay in such cases, our approach is not intended for scenarios where the structure of the data graph changes rapidly.

2.2 Proposed Aggregation Framework

In this section, we describe our proposed framework to support different types of ego-centric aggregate queries. We begin with explaining the notion of an *aggregation overlay graph* and key rationale behind it. We then discuss the execution model and some of the key implementation issues.

2.2.1 Aggregation Overlay Graph

Aggregation overlay graph is a pre-compiled data structure built for a given ego-centric aggregate query, that enables sharing of partial aggregates, selective pre-computation, partial pre-computation, and low-overhead query execution. Given a data graph $\mathcal{G}(V, E)$ and a query $\langle \mathcal{F}, w, \mathcal{N}, pred\rangle$, we denote an aggregation overlay graph for them by $O_{\mathcal{G}}(V'', E'')$.

There are three types of nodes in an overlay graph: (1) the *writer* nodes, denoted by subscript $_w$, one for each node in the underlying graph that is *generating* data, (2) the *reader* nodes, denoted by subscript $_r$, one for each node in V that satisfies $pred$, and (3) the *partial aggregation* nodes (also called *intermediate* nodes). We use the term *aggregation* node to refer to either a reader node or a partial aggregation node, since both of those may perform aggregation. In Figure 1(d), PA_1 and PA_2 are two partial aggregation nodes that are introduced after analyzing the structure of the network and the query. PA_1 corresponds to a partial aggregator that aggregates the inputs a_w, b_w, c_w, and serves e_r, g_r, f_r, c_r, d_r.

For correctness, there can only be one (directed) path from a writer to a reader in an overlay graph (to avoid duplicate contributions from that writer to the aggregate computed for that reader). However, there are two exceptions to this. First, this is not an issue with the so-called *duplicate-insensitive* aggregates like MAX, MIN, UNIQUE. We exploit this by constructing overlays that allow such multiple paths for those aggregates, if it leads to smaller overlays (in most cases, we observed that to be the case).

Second, we allow an overlay to contain what we call *negative* edges to "subtract" such duplicate contributions. A negative edge from a node u to an aggregation node v indicates that the input from u should be "subtracted" (i.e., its contribution removed) from the aggregate result computed by v. Such edges should only be used when the "subtraction" operation is efficiently computable. Although negative edges may appear to lead to wasted work, in practice, adding negative edges (where permissible) can actually lead to significant improvements in the total throughput. We discuss this issue further in Section 3.1.

The overlay graph also encodes pre-computation decisions (also called *dataflow decisions*). Each node in the overlay graph is annotated either *pull* or *push*. If a node is annotated *push*, the partial aggregate that it computes is always kept up-to-date as new updates arrive. The writer nodes are always annotated *push*. For an aggregation node to be annotated *push*, all its input nodes must also be annotated *push*. Analogously, if a node is annotated *pull*, all the nodes downstream of it must also be annotated *pull*. In Figure 1(d), the push and pull decisions are shown with unshaded and shaded nodes respectively. This overlay graph fully pre-computes the query results for nodes e_r and f_r (thus leading to low latencies for those queries); on the other hand, a read on node g_r will incur a high latency since the computation will be done fully on demand.

Note that, we require that the decisions be made for each node in the overlay graph, rather than for each edge. Thus, all the inputs to an aggregation node are either pushed to it, or all the inputs are pulled by it. This simplifies the bookkeeping significantly, without limiting the choices of partial pre-computation. If we desire to pre-compute a partial aggregate over a subset of a node's inputs, a separate partial aggregation node can be created instead. We discuss more details about this in Section 4.

Finally, we note that the aggregation overlay graph can be seen as a pre-compiled query plan where no unnecessary computation or reasoning is performed when an update arrives or a read query is posed. This enables us to handle much higher data rates than would be possible otherwise. We discuss the resulting execution model and related architectural decisions in the following sections.

2.2.2 Execution Model

We begin with describing how new updates and queries are processed using the overlay graph, and briefly discuss some of the implementation issues surrounding multi-threaded execution.

Execution Flow: We describe the basic execution flow in terms of the *partial aggregate objects (PAOs)* that are maintained at various nodes in the overlay graph. A PAO corresponds to a partial aggregate that has been computed after aggregating over a subset of the inputs. The PAO corresponding to a node labeled *push* is always kept up-to-date as new updates arrive in any of the streams it is defined over, or if the sliding windows shift and values drop out of the window. Specifically, the updates originate at the writer nodes, and propagate through the overlay graph as far as indicated by the dataflow decisions on the nodes. The nodes labeled *push* maintain partial state and perform incremental computation to keep their corresponding PAOs up-to-date. On the other hand, no partial state is maintained at the nodes labeled *pull*. When an overlay node u makes a *read* request from another node v upstream of it, if v is labeled *push*, the partial aggregate is returned immediately without delay. On the other hand, if v is labeled *pull*, it issues *read* requests on all its upstream overlay nodes, merges all the PAOs it receives, and returns the result PAO to the requesting node.

Single-threaded vs Multi-threaded Execution: A naive implementation of the above execution model is using a single thread, that processes the *writes* and *reads* in the order in which they are received, finishing each one fully (i.e., pushing the writes as far as required, and computing the results for *reads*) before handling the next one. Although it leads to well-defined and consistent execution, this approach cannot exploit parallelism in the system, and is unlikely to scale. On the other hand, a multi-threaded version requires careful implementation to guarantee correctness. First, the computations on the overlay graph must be made thread-safe to avoid potential state corruption due to race conditions. We can do this either by using thread-safe data structures to store the PAOs or through explicit synchronization. We use the latter approach in our implementation of the aggregates; however, user-defined aggregates may choose either of the two options. A more subtle issue is that of consistency. Consider a read on node a_r in Figure 1(d). It is possible that the result generated contains a more recent update on node f_w, but does not see a relatively older update on node c_w (as f_w is read later than c_w). We ignore the potential for such inconsistencies in this work and plan to address this in future.

We use two thread pools, one for servicing the read requests and one for servicing the write requests. The relative sizes of the two thread pools can be set based on the expected number of reads vs writes; assigning more threads to processing reads may reduce latency, but increases the possibility of stale results.

Further, there are two ways to process a read or a write using multiple threads: (1) a *uni-thread* model, where a thread that picks up a request (read or write) executes it fully before processing a new request, or (2) a *queueing* model, where the tasks are subdivided into micro-tasks at the granularity of the overlay nodes, each of which is responsible for a single PAO operation at an overlay node (update for writes, and computation for reads). Queueing model is likely to be more scalable and result in better throughputs, but the latencies for reads are substantially higher. We follow a hybrid approach, and use uni-thread model for reads and queueing for writes.

2.2.3 User-defined Aggregate API

One of the key features of our system is the ability for the users to define their own aggregate functions. We build upon the standard API for user-defined aggregates for this purpose [19, 36, 24], and briefly describe it here for completeness. The user must implement the following functions.

- INITIALIZE(*PAO*): Initialize the requisite data structures to maintain the partial aggregate state (i.e., PAOs).
- UPDATE(*PAO, PAO_old, PAO_new*): This is the key function that updates the partial aggregate at an overlay node (PAO) given that one of its inputs was updated from *PAO_old* to *PAO_new*.
- FINALIZE(*PAO*): Compute the final answer from the PAO.

Note that, we require the ability to *merge* two PAOs in order to fully exploit the potential for sharing through overlay graphs – this functionality is typically optional in user-defined aggregate APIs.

3. CONSTRUCTING THE OVERLAY

Our overall optimization goal is to construct an overlay graph annotated with pre-computation (dataflow) decisions that maximize the overall throughput, given a data graph and an ego-centric aggregate query. To make the dataflow decisions optimally, we also need information about the expected read (query) and write (update) frequencies for the nodes in the graph. However, these two sets of inputs have inherently different dynamics – the data graph is expected to change relatively slowly, whereas the read/write frequencies are expected to show high variability over time. Hence, we decouple the overall problem into two phases: (1) we construct a compact overlay that maximizes the sharing opportunities given a data graph and a query, and (2) then make the dataflow decisions for the overlay nodes (as we discuss in the next section, we allow the second phase to make restricted local modifications to the overlay). The overlay construction is a computationally expensive process, and we expect that an overlay, once constructed, will be used for a long period of time (with incremental local changes to handle new nodes or edges). On the other hand, we envision re-evaluating the dataflow decisions on a more frequent basis by continuously monitoring the read/write frequencies to identify significant variations.

In this section, we focus on the overlay construction problem. We begin with defining the optimization goal, and present several

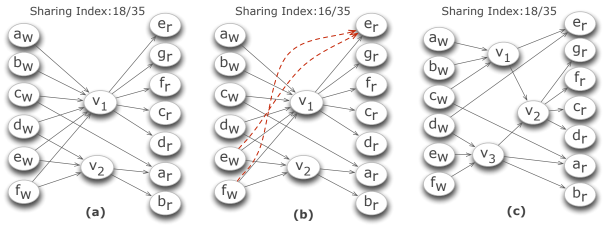

Figure 2: (a) A duplicate-insensitive overlay; (b) An overlay with two negative edges; (c) A multi-level overlay.

scalable algorithms to construct an overlay. We then briefly discuss our approach to handling structural changes to the data graph.

3.1 Preliminaries

As a first step, we convert the given data graph $\mathcal{G}(V, E)$ into an equivalent bipartite graph $A_{\mathcal{G}}(V', E')$, by identifying the query nodes, and the input nodes for each of the query nodes, given the user-provided query (as discussed in Section 2.1). We use the total number of edges in the overlay as our optimization metric, the intuition being that, each edge in the overlay corresponds to a distinct data movement and computation. We justify the use of this somewhat abstract metric by noting that the runtime cost of an overlay is highly dependent on the distribution of the read/write frequencies; for the same query and data graph, the optimal overlays could be wildly different for different distributions of read/write frequencies (which are not available at the overlay construction phase). We believe that the use of an abstract metric that rewards sharing is likely to prove more robust in highly dynamic environments. In future work, we plan to further validate our choice by comparing it against other optimization metrics.

More formally, we define the *sharing index* of an overlay to be:

$$1 - \frac{\textit{\# of edges in the overlay}}{\textit{\# of edges in } A_{\mathcal{G}}}$$

Figure 2 shows three overlays for our running example, and their sharing indexes. Figure 2(a) shows an overlay where there are multiple paths between some reader-writer pairs. As we discussed earlier, such an overlay cannot be used for a duplicate-sensitive aggregate function (like SUM, COUNT, etc.), but for duplicate-insensitive aggregate functions like MAX, it typically leads to better sharing index as well as better overall throughput. The second overlay uses *negative edges* to bring down sharing index. This should only be done for aggregate functions where the subtraction operation is incrementally computable (e.g., SUM, or COUNT). Finally, third overlay is an example of a *multi-level* overlay, and has the lowest sharing index for our running example (without use of negative edges or duplicate paths). In most cases, such multi-level overlays exhibit the best sharing index. Note that multi-level overlays can also be duplicate insensitive or contain negative edges.

The problem of maximizing the sharing index is closely related to the *minimum order bi-clique partition* problem [16], where the goal is to cover all the edges in a bipartite graph using fewest edge-disjoint bicliques. In essence, a biclique in the bipartite graph $A_{\mathcal{G}}$ corresponds to a set of readers that all share a common set of writers. Such a biclique can thus be replaced by a partial aggregation node that aggregates the values from the common set of writers, and feeds them to the readers. In Figure 1(d), node PA_1 corresponds to such a biclique (between writers a_w, b_w, c_w and readers c_r, d_r, e_r, f_r, g_r). Finding bicliques is known to be NP-Hard. Sharing index (SI) is also closely related to the *compression ratio* (CR) metric used in many of the works in *representational graph compression* [10] ; specifically, $CR = 1/(1 - SI)$. However, given the context of aggregation and the possibility of having *negative* and *duplicate-insensitive* edges in the overlay, we differentiate it from compression ratio. The problem of finding a good overlay is also closely related to the problem of *frequent pattern mining* [20, 18] as we discuss in the next section.

3.2 Overlay Construction Algorithms

In this section, we present our algorithms for constructing different types of overlays as outlined in the previous section. Given the NP-Hardness of the basic problem, and further the requirement to scale the algorithms to graphs containing tens of millions of nodes, we develop a set of efficient heuristics to achieve our goal. Our first set of proposed algorithms (called VNM_A, VNM_N, and VNM_D) builds upon a prior algorithm (called VNM) for bipartite graph compression by Buehrer et al. [10], which itself is a adaptation of the well-known FP-Tree algorithm for frequent pattern mining [20, 18]. In our exploratory evaluation, we found that algorithm to offer the best blend of scalability and adaptability for our purposes. Our second algorithm (called IOB) is an incremental algorithm that builds the overlay one reader at a time.

3.2.1 Background: FP-Tree and VNM Algorithms

We begin with a brief recap of the *FP-Tree* algorithm for frequent pattern mining, considered to be one of the most efficient and scalable algorithms for finding frequent patterns. We briefly outline the algorithm using the terminology of readers and writers rather than transactions and items. First, the writers are sorted in the increasing order by their overall frequency of occurrence in the reader input sets, i.e., their out-degree in $A_{\mathcal{G}}$. In our running example, the sort order (breaking ties arbitrarily) would be $\{d_w, c_w, e_w, f_w, a_w, b_w\}$. Then all the reader input lists are rewritten according to that sort order; e.g., we would write the input list of a_r as $\{d_w, c_w, e_w, f_w\}$. Next, the FP-Tree is built incrementally by adding one reader at a time, starting with an empty tree. For the reader under consideration, the goal is to find its longest prefix that matches with a path from the root in the FP-Tree constructed so far. As an example, Figure 3 shows the FP-Tree built after addition of readers a_r, b_r, and e_r. A node in the FP-Tree is represented by: $x_w\{S(x_w)\}$ where x_w is a writer and $S(x_w)$ is a list of readers that contain x_w in their input lists (called *support set*). Now, for reader c_r, the longest prefix of it that matches a path from root is d_w, c_w, e_w, f_w. That reader would then be added to the tree nodes in that path (i.e., to the support sets along that path). If the reader input list contains any additional writers, then a new branch is created in the tree (for e_r a new branch will be created with nodes $a_w\{e_r\}$ and $b_w\{e_r\}$).

Once the tree is built, in the *mining phase*, the tree is searched to find bicliques. A path P in the tree from the root to the node $x_w\{S(x_w)\}$ corresponds to a biclique between the writers corresponding to the nodes in P and the readers in $S(x_w)$. Since our goal is to maximize the number of edges removed from the overlay graph, we search for the biclique that maximizes:

$$benefit(P) = L(P) * |S(P)| - L(P) - |S(P)|,$$

where $L(P)$ denotes the length of the path P and $S(P)$ denotes the support for the last node in the path. Such a biclique can be found in time linear to the size of the FP-Tree. After finding each such biclique, ideally we should remove the corresponding edges (called the *mined edges*) and reconstruct the FP-Tree to find the next biclique with best benefit. Mining the same FP-Tree would still find bicliques but with lower benefit (since the next biclique we find cannot use any of the edges in the previously-output biclique).

We now briefly describe the VNM algorithm [10], which is a highly scalable adaptation of the basic FP-Tree mining approach

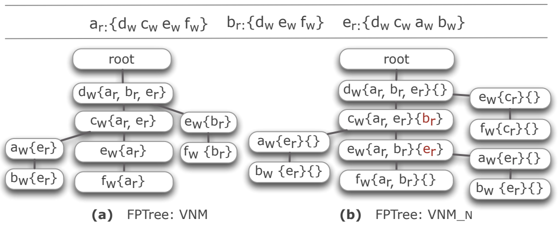

Figure 3: An example of FP-Tree construction for VNM and VNM$_N$: (a) Basic version, (b) FP-Tree with negative edges.

described above; VNM was developed for compressing very large (web-scale) graphs, and in essence, replaces each biclique with a virtual node to reduce the total number of edges. The main optimization of VNM relies on limiting the search space by creating small groups of readers, and looking for bicliques that only involve the readers in one of the groups. This approach is much more scalable than building an FP-Tree on the entire data graph. VNM uses a heuristic based on *shingles* [13, 14] to group the readers. Shingle of a reader is effectively a signature of its input *writers*. If two *readers* have very similar *adjacency lists*, then with high probability, their shingle values will also be the same. In a sense, grouping readers by shingles increases the chance of finding big bicliques (with higher benefit) within the groups. The algorithm starts by computing multiple shingles for each reader, and then doing a lexicographical sort of the readers based on the shingles. The sorted list is then chunked into equal-sized groups of readers, each of which is passed to the FP-Tree algorithm separately. Mining all the reader groups once completes one iteration of the algorithm. The process is then repeated with the modified bipartite graph (where each biclique is replaced with a virtual node) to further compress the graph. Since the virtual nodes are treated as normal nodes in such subsequent iterations, a biclique containing virtual nodes may be replaced with another virtual node, resulting in connections between virtual nodes; in our context, this gives rise to *multi-level overlays* where partial aggregation nodes feed into other partial aggregators.

3.2.2 VNM_A: VNM Adaptive

Our first adaptation of the basic VNM algorithm is aimed at addressing a major deficiency of that algorithm, namely lack of a systematic way to choose the chunk size. Our initial experiments with VNM suggested that the effect of the chunk size on the final compression achieved is highly non-uniform across various graphs like web graphs and social graphs. We noticed that a bigger chunk size typically finds bigger bicliques, but it can't find all big bicliques, especially when there is big overlap in the reader sets of two potential bicliques. This is because the reader sets of two subsequent mining phases in VNM are mutually exclusive. Second, a bigger chunk size makes it harder to find small bicliques, which is especially a problem with later iterations; since many of the original edges have been deleted in the first few iterations, only small bicliques remain in the graph. On the other hand, using a small chunk size from the beginning ignores large bicliques that can deliver huge savings.

To address this problem, we develop an adaptive variation of VNM that uses different chunk sizes for different iterations. For the first iteration, we use a large chunk size (100 in our experiments) and dynamically reduce it for future iterations. For the i^{th} iteration, let c_i denote the chunk size, and let B_i^s denote the sum total of the *benefits* (defined in Section 3.2.1) for all the bicliques found in that iteration with reader set size $= s$ (note that, $s \leq c_i$). We choose $c_{i+1} \leq c_i$ to be the smallest c such that: $\sum_{s \leq c} B_i^s > 0.9 \sum_{s \leq c_i} B_i^s$. Although our algorithm also requires setting two parameter values, our extensive experimental evaluation on many real-world graphs showed that the algorithm is not sensitive to the initial chunk size to within an order of magnitude, and to the second parameter between 0.8 and 1.

3.2.3 VNM_N: VNM with Negative Edges

Next, we present our adaptation to VNM that considers adding negative edges to reduce the overlay size. In essence, we look for *quasi-bicliques* that may be a few edges short of being complete bicliques (this problem is also known to be NP-Hard [23]). For scalability, our algorithm employs the same basic structure as the VNM$_A$ algorithm discussed above (with grouping of readers using shingles); however, we modify the FP-Tree construction and mining algorithms to support negative edges.

Recall that a node in an FP-Tree is represented by $x_w\{S(x_w)\}$ where x_w is a writer and $S(x_w)$ contains the readers that contain x_w in their input lists. To accommodate negative edges, we now represent a node by $x_w\{S(x_w)\}\{S'(x_w)\}$, where $S'(x_w)$ contains readers that do not contain x_w in their input list, but may contain the writers corresponding to the nodes below this node in the FP-Tree. Benefit of a path P in the FP-Tree is now given by:

$$benefit(P) = L(P) * |S(P)| - L(P) - |S(P)| - \sum_P |S'(x_w)|,$$

where the last term captures the number of negative edges along P.

In our proposed algorithm, when an FP-Tree is augmented to include a new reader r, we add r along up to k_1 paths in the FP-Tree that maximize the benefit given the FP-Tree constructed so far. More specifically, we exhaustively explore the FP-Tree in a breadth-first manner, and for each node visited, we compute the benefit of adding r along the path. We then choose up to k_1 paths with the highest benefit and add the reader along those paths. As with the original FP-Tree algorithm, additional branches may have to be created for the remaining writer nodes in r. Figure 3(b) shows an example where both b_r and e_r create two paths in the overlay, one of which uses a negative edge.

Although our algorithm finds the best paths to add the reader along, it runs in time linear to the size of the FP-Tree constructed so far. However, since the FP-Tree, in essence, now encodes information about k_1 times as many readers as it did before, the size of the FP-Tree itself is expected to be larger by about the same factor. To improve efficiency, we stop the breadth-first exploration down a path if more than k_2 negative edges are needed to add r along that path (we set $k_2 = 5$ in our experiments). This optimization has little impact on performance since it is unlikely that quasi-bicliques requiring a large number of negative edges will be beneficial.

3.2.4 VNM_D: Duplicate-insensitive VNM

Next, we discuss our proposed algorithm for finding overlays that exploit the duplicate-insensitive nature of some aggregates and allow for multiple paths between a writer and a reader. There are two natural ways to extend the VNM algorithm for reusing edges in this fashion. First, we can keep the basic structure of the VNM algorithm and modify the FP-Tree algorithm itself to find multiple bicliques in each mining phase, while ignoring the overlap between bicliques. However, by construction, the bicliques mined from a single FP-Tree tend to have very high overlap, and the benefits for additional bicliques found can be very low. It is also not clear how many aggregate nodes to add in a single mining phase; adding all bicliques for which the benefit is non-zero is likely to lead to many partial aggregate nodes, each providing low benefit.

Instead, in our proposed algorithm VNM$_D$, we modify the reader grouping phase itself. In VNM, in each iteration, the readers are grouped into disjoint groups before passing to the FP-Tree construction and mining phase. Instead, we allow the groups of readers to overlap. Specifically, given an overlap percentage p (an algorithm parameter), we allow two consecutive groups of readers to have $p\%$ readers in common. The FP-Tree construction and mining phases themselves are unchanged with the following exceptions. First, instead of representing an FP-Tree node as $x_w\{S(x_w)\}$, we represent it as $x_w\{S^{notmined}(x_w)\}\{S^{mined}(x_w)\}$, where $S^{mined}(x_w)$ contains the readers r such that the edge from x_w to r was present in a previously used biclique. Second, we modify the formula for computing the benefit of a path as follows:

$benefit(P) = L(P) * |S(P)| - L(P) - |S(P)| - \sum_P |S^{mined}(x_w)|$; the last term captures the number of *reused* edges in the biclique.

3.2.5 IOB: Incremental Overlay Building

The overlay constructions algorithms that we have developed so far are all based on identifying sharing opportunities by looking for bicliques in $A_{\mathcal{G}}$. However, to make those algorithms scalable, two heuristics have to be used: one to partition the readers into small groups, and one to mine the bicliques themselves. In essence, both of these focus the search for sharing opportunities to small groups of readers and writers, and never consider the entire $A_{\mathcal{G}}$ at once. Next, we present an incremental algorithm for building the overlay that starts with an empty overlay, and adds one reader at a time to the overlay. For each reader, we examine the entire overlay constructed till that point which, as our experimental evaluation demonstrates, leads to more compact overlays.

We begin with ordering the readers using the shingle order as before, and add the readers one at a time in that order. In the beginning, the overlay graph simply contains the (singleton) writer nodes. Let $\langle r, \mathcal{N}(r)\rangle$ denote the next reader to be added. Let $\langle ovl_n, \mathcal{I}(ovl_n)\rangle$ denote a node in the overlay constructed so far, where $\mathcal{I}(ovl_n)$ is the set of writers whose partial aggregate ovl_n is computing. For reader r, our goal is to reuse as much of the partial aggregation as possible in the overlay constructed so far. In other words, we would like to find the smallest set of overlay nodes whose aggregates can be used to compute the aggregate for r. This problem is essentially the *minimum exact set cover problem*, which is known to be NP-Complete.

We use a standard greedy heuristic commonly used for solving the set cover problem. We start by finding the overlay node that has maximum overlap with $\mathcal{N}(r)$, and restructure the overlay to make use of that overlap. We keep on repeating the same process until all nodes in $\mathcal{N}(r)$ are covered (since the singleton writer nodes are also considered part of the overlay, we can always cover all the nodes in $\mathcal{N}(r)$). Let $\langle v_1, B\rangle$ denote the overlay node that was found to have the highest overlap with the uncovered part, denoted A, of $\mathcal{N}(r)$. If $B \subseteq A$, then we add an edge from v_1 to r, and repeat the process with $A - B$. Otherwise, we restructure the overlay to add a new node $\langle v_1', A \cap B\rangle$, reroute the appropriate incoming edges (i.e., the incoming edges corresponding to the writers in $A \cap B$) from v_1 to v_1', and add a directed edge from v_1' to v_1. We then also add an edge from v_1' to r. If $A - A \cap B$ is non-empty, then we repeat the process to cover the remaining inputs to r.

As with the VNM-based algorithms, we use multiple iterations to improve the overlay. In each iteration (except the 1st iteration), we revisit the decisions made for each of the partial aggregator nodes, and do local restructuring of the overlay if better decisions are found for any of the partial aggregator nodes (using the same set cover-based algorithm as above).

For efficient execution of the algorithm we maintain both a *reverse index* and a *forward index*. For a writer node w, the reverse index tells us which overlay nodes are aggregating w. For example, a_w's reverse index entry will have both v_1 and v_2. Note that even though there is no direct edge from a_w to v_2, a_w's reverse index entry has v_2 because v_2 is effectively aggregating a_w. This index helps us to find the overlay node that provides maximum cover to a set of input nodes using one single scan of the input list. Similarly, for any node n in the overlay, the forward index tells us the input list of n; e.g., v_2's forward index entry will have v_1 and v_3 in it.

Although the above algorithm could be extended to allow for negative edges and/or duplicate paths, we do not discuss those extensions here. This is because, although IOB finds significantly smaller overlays, the overlays tend to be deep (with many levels) and in our experimental evaluation, the end-to-end throughput for the overlays was lower than for the overlays found with the VNM$_A$ algorithm. Thus, although the IOB algorithm is a better algorithm for finding compact overlays and for compressing bipartite graphs, VNM-based algorithms are better suited for our purpose.

3.3 Handling Dynamic Changes

We adapt the basic ideas underlying the IOB algorithm to incrementally update the overlay in response to structural changes (i.e., addition/deletion of nodes/edges) to the data graph. More details can be found in the extended version of the paper [26].

4. MAKING DATAFLOW DECISIONS

Next, we discuss how to make the dataflow (i.e., precomputation) decisions to maximize the total throughput given an overlay network, and the expected read/write frequencies for the nodes. Surprisingly, the problem can be solved optimally in polynomial time. We begin with the preliminaries related to the cost of a dataflow decisions and then provide the formal problem definition and present the analysis along with the algorithms that we propose.

Preliminaries: For each node $v \in V$ in the data graph, let $r(v)$ denote its read frequency (i.e., the number of times a query is issued at node v), let $w(v)$ denote its write frequency (i.e., the number of times v is updated)[1]. Given these, with each node $u \in V''$ in the overlay graph $O_{\mathcal{G}}(V'', E'')$, we associate two numbers, $f_l(u)$ and $f_h(u)$, called *pull frequency* and *push frequency*, respectively. $f_h(u)$ captures the number of times data values would be *pushed* to u if all nodes in the overlay are assigned *push* decisions. Similarly, $f_l(u)$ indicates the number of times data values would be *pulled* from u if all nodes in the overlay are assigned *pull* decisions.

The push and pull frequencies are computed as follows. For computing push frequencies, we start by assigning $f_h(a_w) = w(a_w)$ for all writer nodes a_w, and then propagate the push frequencies from left to right (downstream). For an aggregation node or a reader node u, $f_h(u)$ is computed by summing up the push frequencies for all nodes that are immediately upstream of u. Similarly, the pull frequencies are computed by starting with the reader nodes, then recursively computing the pull frequencies for the rest of the nodes. Figure 4(i)-(iii) illustrates this with an example that we also use to show how our algorithm makes the dataflow decisions.

Push and Pull Costs: As discussed before, a *push* decision on a node implies that the aggregate corresponding to that node will be (incrementally) precomputed and will be available for immediate consumption. On the other hand, a *pull* decision on a node implies that the aggregate will be computed on demand when the node is read. To reason about the tradeoff between push and pull, we need to be able to compute the cost of a push or a pull. This cost typically depends on the nature of the aggregate, and the type and the size of the sliding window [6]. We capture these costs as two functions:

[1] See Table 1 for a summary of notation.

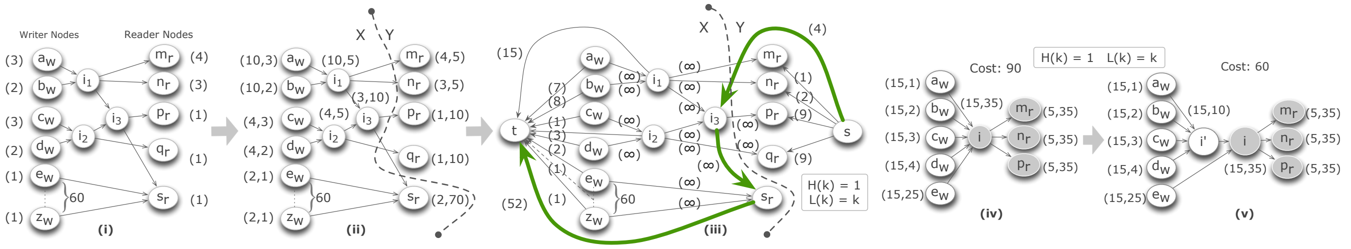

Figure 4: (i) An example overlay annotated with read/write frequencies; (ii) Computing (*pull*, *push*) frequencies; (iii) Construction of the *s-t* augmented graph (with the annotations denoting the edge weights); (iv-v) Splitting a node based on push-pull frequencies.

$H(k)$ denotes the average cost of one push for an aggregation node with k inputs, and $L(k)$ denotes the average cost of one pull for that node. For example, for a SUM aggregate node, we expect $H(k) \propto 1$ and $L(k) \propto k$, whereas for a MAX aggregate node, if we use a priority queue for handling incremental updates, then $H(k) \propto \log_2(k)$ and $L(k) \propto k$. To handle sliding windows, we implicitly assign w inputs to each writer where w is the average number of values in the sliding window at a writer – thus if the sliding window is of size 10, then $PUSH$ and $PULL$ costs of the writer node will be $H(10)$ and $L(10)$ respectively. We assume $H()$ and $L()$ are either provided, or are computed through a calibration process where we invoke the aggregation function for a range of different inputs and learn the $H()$ and $L()$ functions.

Problem Definition: The dataflow decisions made by a solution induce a *node partition*, denoted $(X, Y), X \cap Y = \phi$, on the overlay graph, where X contains nodes that are designated *push*, Y contains nodes designated *pull* (Figure 4(ii)). Since all nodes upstream of a *push* node must also be designated *push* (and similarly all nodes downstream of a *pull* node must also be *pull*), the partition induced by any consistent set of dataflow decisions must satisfy the constraint that there is no edge from a node in Y to a node in X.

For an overlay node v, let $PUSH(v) = f_h(v) * H(deg(v))$ denote the cost incurred if it is designated a *push* node, let $PULL(v) = f_l(v) * L(deg(v))$ denote the cost if it is a *pull* node. Although the push/pull decisions cannot be made for the nodes independently (because of the aforementioned constraint), $PUSH()$ and $PULL()$ costs can be computed independently; this is because the computations that happen at a node when it is invoked, do not depend on the dataflow decisions at its input or output nodes. Thus, to minimize the total computational cost, our goal reduces to finding an (X, Y) partition of the overlay (with no edges going from Y to X) that minimizes: $\sum_{v \in X} PUSH(v) + \sum_{v \in Y} PULL(v)$.

Query Latencies: Another consideration in making dataflow decision is the impact on query *latencies*. Throughput maximization may lead to higher use of *pull* decisions, especially if reads are less frequent than writes, that may result in high query latencies. As we show in Section 5, because our system is entirely in-memory and does not need to do distributed network traversals, the query latencies are quite low even in the worst-case. In future work, we plan to investigate latency-constrained optimization as well as understand the interplay between throughput and latency better.

Algorithm: We design an algorithm for a slightly more general problem, that we describe first. We are given a directed acyclic graph $H(H_V, H_E)$, where each vertex $v \in H_V$ is associated with a weight $w(v)$; $w(v)$ may be negative. For ease of exposition, we assume that $\forall v, w(v) \neq 0$. We are asked to find a graph partition (X, Y), such that there are no edges from Y to X, that maximizes: $\sum_{v \in X} w(v) - \sum_{v \in Y} w(v)$. Note that, the solution is trivially $(X = H_V, Y = \phi)$ if all node weights are positive. We also note that, the metric has the maximum possible value if all nodes with $w(v) < 0$ are assigned to Y, all nodes with $w(v) > 0$ to X. However, that particular assignment may not guarantee that there are no edges from Y to X.

To reduce our problem to this problem, we set:

$$w(v) = f_l(v)L(deg(v)) - f_h(v)H(deg(v)) = PULL(v) - PUSH(v)$$

That is, the weight of node v is the "*benefit*" of assigning it a *push* decision (which is negative if $PULL(v) < PUSH(v)$). Then:

$$\begin{aligned} & \sum_{v \in X} w(v) - \sum_{v \in Y} w(v) \\ &= \sum_{v \in X} (PULL(V) - PUSH(v)) - \sum_{v \in Y} (PULL(V) - PUSH(v)) \\ &= \underline{\sum_{v \in H_V} (PULL(v) + PUSH(v))} - 2(\sum_{v \in X} PUSH(v) + \sum_{v \in Y} PULL(v)) \end{aligned}$$

Since the underlined term is a constant, maximizing this is equivalent to minimizing $\sum_{v \in X} PUSH(v) + \sum_{v \in Y} PULL(v)$.

To solve this more general problem, we construct an edge-weighted graph $H'(H'_V, H'_E)$ from $H(H_V, H_E)$ (in practice, we do not make a copy but rather augment H in place). H'_V contains all the vertices in H_V and in addition, it contains a *source* node s and a *sink* node t (nodes in H' are unweighted). Similarly, H'_E contains all the edges in H_E, with edge weights set to ∞. Further, for each $v \in H_V$ such that $w(v) < 0$, we add a directed edge in H' from s to v with weight $w'(s, v) = -w(v)$. Similarly for $v \in H_V, s.t.\ w(v) > 0$, we add a directed edge in H' from v to t with weight $w'(v, t) = w(v)$ (see Figure 4(iii) for an example).

We note that, this construction may seem highly counter-intuitive, since a lot of nodes in H' have either no outgoing or no incoming edges and there are few, if any, directed paths from s to t. In fact, the best case scenario for the algorithm is that: *there is no directed path from s to t*. This is because, a path from s to t indicates a *conflict* between two or more nodes. The highlighted path form s to t in Figure 4(iii) provides an example. The best decision for node i_3 in isolation would be *pull* ($PULL(i_3) = 6, PUSH(i_3) = 10$), but that for s_r is *push* because of its high in-degree and because $L(k) = k$ ($PULL(s_r) = 2 * 60 = 120, PUSH(s_r) = 70$). However, a *pull* on i_3 would force a *pull* on s_r, hence both of them cannot be assigned the optimal decision in isolation.

After constructing H', we find an s-t directed min-cut in this directed graph, i.e., a set of edges $C \in H'_E$ with minimum total edge-weight, such that removing those edges leaves no directed path from s to t. Let Y denote the set of nodes in H' reachable from s after removing the edges in C (excluding s), let X denote the set of remaining nodes in H' (excluding t).

THEOREM 4.1. *(X, Y) is a node partition of H s.t. there are no edges from Y to X, $\sum_{v \in X} w(v) - \sum_{v \in Y} w(v)$ is maximized.*[2]

We use the Ford-Fulkerson algorithm to construct an s-t maxflow in H', and use it to find the optimal (X, Y) partition of H.

[2] Proofs can be found in the extended version of the paper [26].

Pre-processing: Although the above algorithm runs in polynomial time, it is not feasible to run max-flow computations on the graphs we expect to see in practice. However, a simple pre-processing pruning step, run on H before augmenting it, typically results in massive reduction in the size of the graph on which the max-flow computation must be run.

Consider node a_w in the example graph in Figure 4(ii). The best decision for that node by itself is a *push* decision (since $PUSH(a_w) = 3 < PULL(a_w) = 10$). Since there is no node upstream of a_w (which is a writer node), we can assign this node a *push* decision without affecting decisions at any other node (any node downstream of a_w can still be assigned either decision), and remove it from the graph. Similarly we can assign push decision to node b_w and remove it from H. After that, we can see that node i_1 can also now be assigned a *push* decision (optimal for it in isolation) without affecting any other node. Similarly, we can assign *pull* decisions to nodes m_r, n_r, p_r, q_r and remove them by an analogous reasoning.

We now state the pruning rules, which are applied directly to H (i.e., before constructing the augmented graph): (P1) recursively remove all nodes v such that $w(v) > 0$ and v has no incoming edges, and assign them *push* decisions, (P2) recursively remove all nodes v such that $w(v) < 0$ and v has no outgoing edges, and assign them *pull* decisions. This pruning step can be applied in linear time over the overlay graph. We apply the above max-flow-based algorithm to each of the connected components separately.

THEOREM 4.2. *Use of pruning rules P1 and P2 does not compromise optimality.*

Greedy Alternative to the Max-flow-based Algorithm: We also sketch a simpler greedy algorithm for making dataflow decisions (we did not encounter a need for this algorithm in our extensive experimental evaluation). We traverse the overlay graph starting from the writers in a breadth-first manner, assigning each node v the optimal decision (i.e., a *push* decision if $PUSH(v) < PULL(v)$, and *pull* otherwise), with one exception: if a node should be assigned a *push* decision, but some of its input nodes are assigned *pull* decisions, we make a greedy cost-based decision among the two choices (this is only done if no nodes further upstream from v are assigned a *pull* decision). A detailed exposition can be found in [26]. This greedy algorithm runs in time linear in the number of edges (each edge is processed at most twice), and is thus highly efficient.

Partial Precomputations by Splitting Nodes: Making decisions on a per-node basis can lose out on a significant optimization opportunity – based on the push and pull frequencies, it may be beneficial to partially aggregate a subset of the inputs to an aggregate node. Figure 4(iv)-(v) shows an example. Here, because of the low write frequencies for inputs a_w, b_w, c_w, and d_w for aggregator node i, it is better to compute a partial aggregate over them, but compute the full aggregate (including e_w) only when needed (i.e., on a read).

One option is to make pre-computation decisions on a per-edge basis. However, that optimization problem is much more challenging because the cost of an incremental update for an aggregate node depends on how many of the inputs are being incrementally aggregated and how many on demand; thus the decisions for different edges are not independent of each other. Next we sketch an algorithm that achieves the same goal, but in a more scalable manner.

For every node v in the overlay graph, we consider splitting its inputs into two groups. Let f denote the pull frequency for v, and let $f_1, ..., f_k$ denote the push frequencies of its input nodes, sorted in the increasing order. For every prefix $f_1, ..., f_l$, of this sequence, we compute: $\sum_{i \leq l} f_i H(l) + f \times L(l)$. We find the value of l that minimizes this cost; if $l \neq 0$ and $l \neq k$, we construct a new node v' that aggregates the inputs corresponding to frequencies $f_1, ..., f_l$, remove all those inputs from v, add v' as an input to v. As we show in our experimental evaluation, this optimization results in significant savings in practice.

Adapting the Dataflow Decisions: Most real-world data streams, including graph data streams, show significant variations in read/write frequencies over time. We propose and empirically evaluate, a simple adaptive scheme to handle such variations. For a subset of the overlay nodes (specified below), we monitor the observed push/pull frequencies over recent past (the window size being a system parameter). If the observed push/pull frequencies at a node are significantly different than the estimated frequencies, then we reconsider the dataflow decision just for that node and change it if deemed beneficial. Dataflow decisions can be unilaterally changed in such a manner only for: *pull* nodes all of whose upstream nodes are designated *push*, and *push* nodes all of whose downstream nodes are designated *pull* (we call this the *push/pull frontier*). Hence, these are the only nodes for which we monitor push/pull frequencies (it is also easier to maintain the push/pull frequencies at these nodes compared to other nodes). Techniques for more sophisticated adaptive schemes is a rich area which we plan to pursue in future.

5. EVALUATION

In this section, we present a extensive experimental evaluation using several real-world information networks. Our results show that our approach results in orders of magnitude improvements in the end-to-end throughputs over baselines, and that our overlay construction algorithms are effective at finding compact overlays.

5.1 Experimental Setup

We ran our experiments on a 2.2GHz, 24-core Intel Xeon server with 64GB of memory, running 64-bit Linux. Our prototype system is implemented in Java. We use a set of dedicated threads to play back the write and read traces (i.e., to send updates and queries to the system), and a thread pool to serve the read and write queries.

Datasets and Query Workload: We evaluated our approach on several real-world information networks, and here we report results for 4 of them[3]: (1) LiveJournal (*soc-LiveJournal1*: 4.8M nodes/69M edges), (2) Google+ social circles (*ego-Gplus*:107k/13M), (3) *EU2005* Web Graph (862k /19M), and (4) *UK2002* Web Graph (18.5M /298M).

We report results for three ego-centric aggregate queries: SUM, MAX, and TOP-K, all specified over 1-hop neighborhoods. SUM and MAX queries ask us to compute the total sum and the max over the input values respectively. TOP-K asks for the k most *frequent* values among the input values, and is a holistic aggregate [24].[4]

Since the user activity patterns (i.e., read/write frequencies) are not available for any real-world network that we are aware of, we generate those synthetically using a Zipfian distribution; event rates in many applications like tweets in Twitter, page views in Yahoo!'s social platform have been shown to follow a Zipfian distribution [30, 9]. Further, we assume that the read frequency of a node is linearly related to its write frequency; we vary the write-to-read ratio itself to understand its impact on the overall performance. For some of the experiments, we used real network packet traces to simulate user activity [5]: (1) EPA-HTTP, and (2) UCB Home IP Web Traces.

[3] First two are available at http://snap.stanford.edu/data/index.html, and the latter two at http://law.di.unimi.it/.

[4] In other words, TOP-K is a generalization of *mode*, not *max*.

[5] Available at http://ita.ee.lbl.gov/html/traces.html.

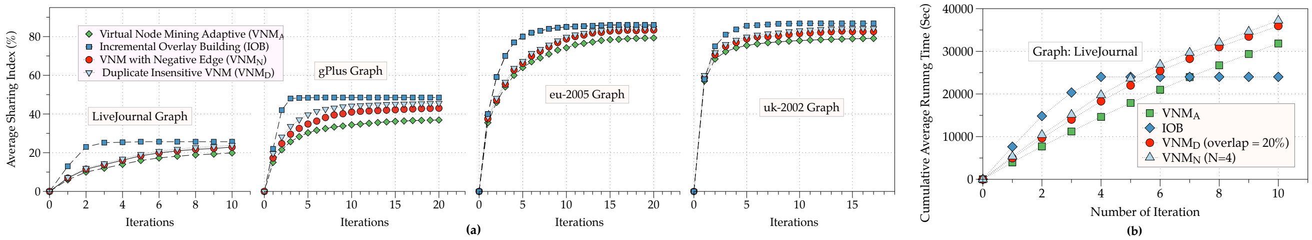

Figure 5: (a) Comparing overlay construction algorithms on real networks; (IOB should not be directly compared against VNM$_N$ or VNM$_D$ since it doesn't use negative edges or duplicate paths); (b) Running time comparison of the overlay construction algorithms.

Evaluation Metric: Our main evaluation metric is the *end-to-end throughput of the system*, i.e., the total number of read and write queries served per second. This metric accounts for the side effects of all potentially unknown system parameters whose impact might not show up for a specifically designed metric, and thereby reveals the overall efficacy of the system. When comparing the overlay construction algorithms, we also use the following metrics: sharing index (SI), memory consumption, and running time.

Comparison Systems or Algorithms: For overlay construction, we compare five algorithms: VNM, VNM$_A$, VNM$_N$, VNM$_D$, and IOB. For overall throughput comparison, we compare three approaches: (1) *all-pull*, where all queries are evaluated on demand (i.e., no sharing of aggregates and no pre-computation), (2) *all-push*, where all aggregates are pre-computed, but there is no sharing of partial aggregates, and (3) *dataflow-based overlay*, i.e., our approach with sharing of aggregates and selective pre-computation. We chose the baselines based on industry standards: *all pull* is typically seen in social networks, whereas *all push* is more prevalent in data streams and complex event processing (CEP) systems.

5.2 Overlay Construction

Sharing Index: First we compare the overlay construction algorithms with respect to the *average sharing index* achieved per iteration, over 5 runs (Figure 5(a)). As we can see, IOB finds more compact overlays (we observed this consistently for all graphs that we tried). The key reason is that: IOB considers the entire graph when looking for sharing opportunities, whereas the VNM variations consider small groups of readers and writers based on heuristical ordering of readers and writers. Note that, IOB should only be compared against VNM$_A$, and not VNM$_N$ or VNM$_D$, since it doesn't use negative edges or duplicate paths. We also note that, for IOB, most of the benefit is obtained in first few iterations, whereas the VNM-based algorithms require many iterations before converging. Further, the overlays found by VNM$_N$ and VNM$_D$ are significantly better than those found by VNM$_A$. This validates our hypothesis that using negative edges and reusing mined edges, if possible, results in better overlays. Another important trend that we see here is that the sharing indexes for web graphs are typically much higher those for the social graphs. Kumar et al. also notice similar difficulties in achieving good structural compression in social networks [13].

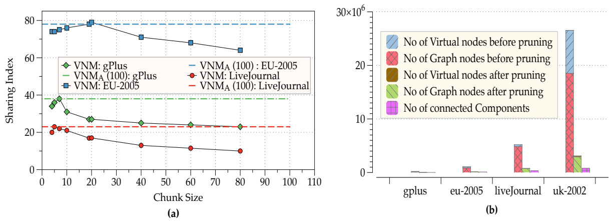

Figure 6: (a) Effect of chunk size on VNM; (b) Benefits of pruning before running maxflow.

Comparing VNM and VNM$_A$: Figure 6(a) shows SI achieved by our adaptive VNM$_A$ algorithm and by VNM$_A$ as the chunk size is varied. As we can see, VNM is highly sensitive to this parameter, whose optimal value is quite different for different data graphs. On the other hand, VNM$_A$ is able to achieve as compact an overlay (in some cases, slightly better) as the best obtained by VNM.

Running time and Memory Consumption: Figure 5(b) shows the running time for the different construction algorithms with the increasing number of iterations for the LiveJournal graph. As we can see IOB takes more time for first few iterations, but is overall faster than the VNM$_A$ and its variations since it converges faster. As expected, both VNM$_N$ and VNM$_D$ take more time per iteration than VNM$_A$. We also compared the total memory consumption of the overlay construction algorithms (not plotted). For LiveJournal, VNM$_A$ and its variations used approximated 4GB of memory, whereas IOB used 8GB at its peak; this is not surprising considering that IOB needs to maintain additional global data structures.

Additional experiments [26]: We found that IOB creates a deeper overlay with average depth of 4.66 (vs 3.44 for VNM$_A$), where overlay depth for a reader is defined to be the length of the longest path from one of its inputs to itself. We also found that for VNM$_N$ the number of negative edges has a significant impact on the sharing index, however the benefit diminishes beyond 3-4 negative edges.

5.3 Dataflow Decisions

Effectiveness of Pruning: Figure 6(b) shows the effectiveness of our pruning strategy to reduce the input to the max-flow algorithm. We have plotted the result for a read/write ratio of 1:1, as intuitively pruning is expected to be least effective in this case. Results for other read/write ratios show similar trend and can be found in the extended version [26]. Each vertical bar in the figure has been divided to show the composition of intermediate overlay nodes and original graph nodes, before and after pruning the overlays that we got using VNM$_A$. We get similar results for other overlay construction algorithms as well. The pruning step not only reduces the size of the graphs (to below 14% in all cases), but the resulting graphs are also highly disconnected with many small connected components, leading to low running times for the max-flow computations.

Baseline for Dataflow Decisions: Figure 8(b) shows the effectiveness of the dataflow decisions on the overlay. In this experiment we kept the number of threads (12) and read/write ratio (1:1) of the queries fixed and computed the average throughput for: (a) overlay with all push, (b) overlay with dataflow decisions, and (c) overlay with all pull. As we can see, for all aggregate functions, overlay with optimal dataflow performs much better than overlay with all pull and all push thereby justifying our hypothesis. We observed similar results for other read/write ratios as well.

Adaptive Dataflow Decisions on a Real Trace: Figure 8(a) shows the ability of our proposed adaptive scheme to adapt to varying read/write frequencies. We used the EPA-HTTP network packet

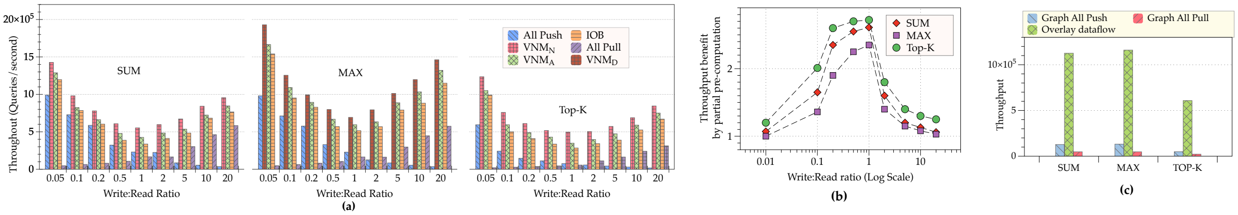

Figure 7: (a) End-to-end throughput comparison for different aggregate functions for the LiveJournal graph, with 24 threads; (b) Benefits of partial pre-computation through node splitting; (c) Throughput comparison for 2-hop aggregates.

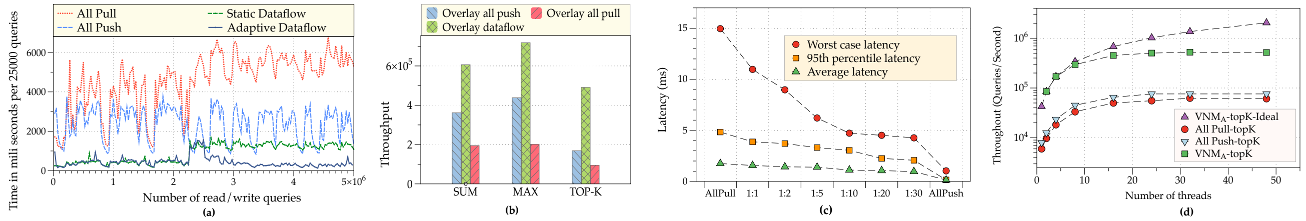

Figure 8: (a) Effect of workload variations on different approaches; (b) Baseline to motivate dataflow decisions; (c) Read latency for different push:pull cost; (d) Effect of increasing parallelism on throughput.

trace to simulate read/write activity for nodes. We used average read/write frequencies of the nodes to make static dataflow decisions. At a half-way point, we modified the read/write frequencies by increasing the read frequencies of a set of nodes with the highest read latencies till that point. As we can see, the static dataflow decisions turn out to be significantly suboptimal once this change is introduced. However, our simple adaptive approach is able to quickly adapt to the new set of read/write frequencies.

5.4 Throughput Comparison

Varying Read-Write Ratio: Figure 7(a) shows the results of our main end-to-end throughput comparison experiments for the three ego-centric aggregate queries. We plot the throughputs for the two baselines as well as for the overlays constructed by the different algorithms, as the write/read ratio changes from 0.05 (i.e., the workload contains mostly reads) to 20. As we can see, the overlay-based approaches consistently outperform the baselines in all scenarios. For the more realistic write/read ratios (i.e., around 1), the throughput improvement over the best of the two baselines is about a factor of 5 or 6. For read-heavy workloads, the overlay-based approach is multiple orders of magnitude better than the *all-pull* approach, and about a factor of 2 better than the *all-push* approach, whereas the reverse is true for the write-heavy workloads.

Comparing different aggregate functions, the performance improvements are much higher for the computationally expensive TOP-K aggregate. In some sense, simple aggregates like SUM and MAX represent a worst case for our approach; the total time spent in aggregate computation (which our approach aims to reduce through sharing) forms a smaller fraction of the overall running time.

Comparing the different overlay construction algorithms, we note that VNM$_N$ shows significant performance improvements over the rest of the overlay construction algorithms, whereas IOB is typically the worst; the higher depth of the overlay increases the total amount of work that needs to be done for both writes and reads.

Effect of Splitting Aggregate Nodes: Figure 7(b) shows the effect of our optimization of splitting an overlay aggregate node based on the push frequencies of its inputs (Section 4) on the LiveJournal graph. As we can see, for all the aggregate functions, this optimization increases the throughput by more than a factor of 2 when write-to-read ratio is around 1. In the two extreme cases (i.e., very low or very high write-to-read ratios) where the decisions are either all push or all pull, this optimization has less impact.

Latency: Figure 8(c) shows the *worst case*, *95th percentile*, and *average* latency for the read queries for TOP-K as the push cost to pull cost ratio is varied. Here we used the network packet trace EPA-HTTP to simulate read/write activity. Since the number of distinct IP addresses in the trace is much smaller than the number of nodes in the (LiveJournal) graph, we randomly split the trace for each IP address among a set of nodes in the graph. We eliminated contention by ensuring that each query or update runs in isolation. As we can see, increasing the *pull cost* bring down the read latencies, as *pushes* get favored while making dataflow decision. We also note that the worst-case latencies in our system are quite low.

Two-hop Aggregates: Figure 7(c) shows the throughput comparison for different aggregates specified over 2-hop neighborhoods for VNM$_A$ overlay compared to all pull and all push; we used the write-to-read ratio of 1 over the LiveJournal graph. The relative performance of the overlay approach compared to all push or all pull is better for 2-hop aggregates than 1-hop aggregate, which can be attributed to better sharing opportunities in such queries.

Parallelism: Figure 8(d) shows how the throughput varies as we increase the number of threads serving the read and write requests for the three approaches; we use the TOP-K query over the LiveJournal graph, with write-to-read ratio of 1. Because of the synchronization overheads, we don't see perfect scaleup (note that the y-axis is in log-scale); for all three approaches, the throughput increases steadily till about 24 threads, and then plateaus out (our machine has 24 cores with hyperthreading enabled).

6. RELATED WORK

Of the prior work on data stream management, the work on evaluating continuous aggregate queries over data streams is most closely related to our work [5, 3, 22, 7]. However, the sharing opportunities in ego-centric aggregate computation over graphs are fundamentally different and have not been studied in that prior work. Further, most of the prior work on evaluating continuous aggregates has only considered the *all-push* model of query evaluation. There has also been much work on aggregate computation in sensor networks and distributed databases, some of which has considered sharing of partial aggregates (e.g., [32, 31, 24]). However the primary optimization goal in that work has been minimizing communication cost during distributed execution, and hence the techniques developed are quite different. Several lines of work have considered the problems in deciding when to push vs pull based on monitoring read/write frequencies, in the context of replication in distributed data management systems (e.g., [34, 27]), and publish-subscribe systems (e.g., [30]). That work has typically focused on minimizing communication cost in distributed settings rather that the CPU cost of computation. Recently, several researchers have looked at the problem of executing subgraph pattern matching queries over streaming graph data (e.g., [33]). Two extensions to SPARQL have also been proposed in recent work for specifying continuous queries over streaming RDF data [8, 4]. There is also much work on streaming algorithms for specific problems like *counting triangles*, PageRank computation, sketching, etc. Two very recent works, Kineograph [12] and GraphInc [11], also address continuous analytics over graphs. Ego-centric analysis of information networks has been getting increasing attention in recent years in *network science* community; here the main focus is on structural analysis of a node's neighborhood [21] as well as on answering specialized pattern matching queries [28]. In a recent work, Yan et al. [35] investigate neighborhood aggregation queries aimed at finding top-k nodes (w.r.t. aggregates over their h-hop neighborhood) in the entire graph. They develop pruning techniques by noting that the aggregate values of two adjacent nodes are similar. However, none of that prior work considers execution of a large number of ego-centric aggregate queries, or exploit many of the optimization opportunities (e.g., aggressive sharing, pre-computations, adaptivity, etc.) that are crucial to handle very high data-rate streams.

7. CONCLUSIONS

In this paper, we presented the design of a continuous query processing system to efficiently process large numbers of ego-centric aggregation queries over highly dynamic, large-scale graphs. Our definition of an ego-centric aggregation query is very general, and captures a range of querying and analytics tasks including personalized trend detection, anomaly or event detection, even complex real-time analytics over neighborhoods in the graph. We proposed a general framework that supports user-defined aggregate queries and enables efficient evaluation of such queries over highly dynamic graphs; we also developed novel scalable algorithms for exploiting sharing opportunities and for making dataflow decisions based on expected activity patterns. Our system is able to handle graphs containing 320M nodes and edges on a single machine with 64GB of memory, achieving update and query throughputs over 500k/s. With the large-memory, many-core machines that are available today, we expect such a centralized approach to be sufficient in most application domains. However, our approach is also naturally parallelizable through use of standard graph partitioning-based techniques. The *readers* can be partitioned in a disjoint fashion over a set of machines, and for each machine, an overlay can be constructed for the readers assigned to that machine; the writes for each *writer* would be sent to all the machines where they are needed.

Acknowledgments: This work was supported by NSF under grant IIS-1319432, by Air Force Research Lab (AFRL) under contract FA8750-10-C-0191 and by an IBM Faculty Award.

8. REFERENCES

[1] F. Abel, Q. Gao, G.-J. Houben, and K. Tao. Analyzing user modeling on twitter for personalized news recommendations. In *UMAP*. 2011.

[2] L. Akoglu, M. McGlohon, and C. Faloutsos. Oddball: Spotting anomalies in weighted graphs. In *KDD*. Springer, 2010.

[3] L. Al Moakar. *Class-Based Continuous Query Scheduling in Data Stream Management Systems*. PhD thesis, Univ. of Pittsburgh, 2013.

[4] D. Anicic, P. Fodor, S. Rudolph, N. Stojanovic. EP-SPARQL: a unified language for event processing and stream reasoning. *WWW*, 2011.

[5] A. Arasu, S. Babu, and J. Widom. The CQL continuous query language: semantic foundations and query execution. *VLDB*, 2006.

[6] A. Arasu and J. Widom. Resource sharing in continuous sliding-window aggregates. In *VLDB*, 2004.

[7] B. Babcock, M. Datar, and R. Motwani. Load Shedding for Aggregation Queries over Data Streams. In *ICDE*, 2004.

[8] D. F. Barbieri, D. Braga, S. Ceri, and M. Grossniklaus. An execution environment for C-SPARQL queries. In *EDBT*, 2010.

[9] L. Breslau, P. Cao, L. Fan, G. Phillips, S. Shenker. Web caching and Zipf-like distributions: Evidence and implications. *INFOCOM*, 1999.

[10] G. Buehrer and K. Chellapilla. A scalable pattern mining approach to web graph compression with communities. In *WSDM*, 2008.

[11] Z. Cai, D. Logothetis, and G. Siganos. Facilitating real-time graph mining. In *CloudDB*, 2012.

[12] R. Cheng et al. Kineograph: taking the pulse of a fast-changing and connected world. In *EUROSYS*, 2012.

[13] F. Chierichetti, R. Kumar, S. Lattanzi, M. Mitzenmacher, A. Panconesi, P. Raghavan. On compressing social networks. *SIGKDD*, 2009.

[14] E. Cohen et al. Finding Interesting Associations without Support Pruning. In *ICDE*, 2000.

[15] M. Everett and S. Borgatti. Ego network betweenness. *Social networks*, 2005.

[16] T. Feder and R. Motwani. Clique partitions, graph compression and speeding-up algorithms. In *STOC*, 1991.

[17] I. Guy, N. Zwerdling, I. Ronen, D. Carmel, and E. Uziel. Social media recommendation based on people and tags. In *SIGIR*, 2010.

[18] J. Han, J. Pei, and Y. Yin. Mining frequent patterns without candidate generation. In *SIGMOD*, 2000.

[19] J. M. Hellerstein et al. The MADlib analytics library: or MAD skills, the SQL. *VLDB*, 2012.

[20] A. Inokuchi, T. Washio, and H. Motoda. An Apriori-Based Algorithm for Mining Frequent Substructures from Graph Data. In *PKDD*, 2000.

[21] J. M. Kleinberg, S. Suri, E. Tardos, and T. Wexler. Strategic network formation with structural holes. *SIGecom*, 2008.

[22] S. Krishnamurthy, C. Wu, and M. J. Franklin. On-the-fly sharing for streamed aggregation. In *SIGMOD*, 2006.

[23] X. Liu, J. Li, and L. Wang. Quasi-bicliques: Complexity and binding pairs. In *Computing and Combinatorics*. Springer, 2008.

[24] S. Madden, M. J. Franklin, J. M. Hellerstein, W. Hong. TAG: a Tiny Aggregation service for Ad-Hoc sensor networks. In *OSDI*, 2002.

[25] J. J. McAuley and J. Leskovec. Learning to discover social circles in ego networks. In *NIPS*, 2012.

[26] J. Mondal and A. Deshapnde. EAGr: Supporting Continuous Ego-centric Aggregate Queries over Large Dynamic Graphs. *arXiv preprint arXiv:1404.6570*, 2014.

[27] J. Mondal and A. Deshpande. Managing large dynamic graphs efficiently. In *SIGMOD*, 2012.

[28] W. E. Moustafa, A. Deshpande, and L. Getoor. Ego-centric graph pattern census. In *ICDE*, 2012.

[29] B. A. Prakash et al. BGP-Lens: Patterns and anomalies in internet routing updates. In *SIGKDD*, 2009.

[30] A. Silberstein, J. Terrace, B. F. Cooper, R. Ramakrishnan. Feeding frenzy: selectively materializing users' event feeds. *SIGMOD*, 2010.

[31] A. Silberstein and J. Yang. Many-to-Many Aggregation for Sensor Networks. In *ICDE*, 2007.

[32] N. Trigoni, Y. Yao, A. J. Demers, J. Gehrke, and R. Rajaraman. Multi-query Optimization for Sensor Networks. In *DCOSS*, 2005.

[33] C. Wang and L. Chen. Continuous subgraph pattern search over graph streams. In *ICDE*, 2009.

[34] O. Wolfson, S. Jajodia, and Y. Huang. An adaptive data replication algorithm. *TODS*, 1997.

[35] X. Yan, B. He, F. Zhu, and J. Han. Top-K aggregation queries over large networks. In *ICDE*, 2010.

[36] Y. Yu, P. K. Gunda, and M. Isard. Distributed aggregation for data-parallel computing: interfaces and implementations. In *SIGOPS*, 2009.